

Kinetic Degradation of IMiD Molecular Glues and Their Target Families

Authors

Paul Held and Jason Greene,
Agilent Technologies, Inc.
Winooski, VT, USA

Sarah D. Mahan, Danette L. Daniels,
and Thomas Machleidt
Promega Corporation
Madison, WI, USA

Abstract

Targeted protein degradation of disease-causing proteins has proven to be a powerful therapeutic approach. The ability to monitor the specificity of degradation amongst related target classes at endogenous protein levels, continuously in live cells, is critical for understanding the efficacy and mechanism of these compounds. This application note shows the automation of parallel degradation and viability screening of several key immunomodulatory drug (IMiD) molecular glue targets, IKZF1 (Ikaros), GSPT1, and IKZF2 (Helios) with various IMiDs using the Promega Nano-Glo HiBiT technology, in conjunction with the Agilent BioTek BioSpa 8 automated incubator and the Agilent BioTek Synergy Neo2 hybrid multimode reader.

Introduction

Targeted protein degradation of disease-causing proteins has proven to be a powerful therapeutic approach, particularly in the field of oncology, using small molecule IMiDs, termed “molecular glues”.¹⁻⁴ Thalidomide represents the first compound in this molecular class. It was first developed in the 1950s as an antiemetic, but it was found to be teratogenic and subsequently taken off the market. The teratogenic properties of thalidomide stimulated the exploration of its anticancer properties. The primary cellular target of thalidomide was identified to be cereblon (CRBN), a substrate receptor of cullin-RING ligase 4 (CRL4).⁵ IMiDs target CUL4-RBX1-DDB1-CRBN (CRL4CRBN) E3 ligase complex to induce the ubiquitination and proteasomal degradation of Ikaros family zinc finger proteins (IKZF family), Ikaros (IKZF1) and Aiolos (IKZF3), which are the lymphoid transcription factors essential for myeloma cell survival.^{6,7,8} IMiDs, such as thalidomide, contain a conserved glutarimide ring and a variable phthaloyl ring. The glutarimide ring interacts with a conserved hydrophobic pocket of CRBN.⁹⁻¹¹ Several derivatives have since been developed to improve efficacy.

The ability to monitor the specificity of degradation amongst related target classes, as well as endogenous protein levels continuously in live cells, is critical for understanding the efficacy and mechanism of therapeutic compounds. The application of the HiBiT CRISPR endogenous tagging provides a highly sensitive and quantitative approach for live cell detection of endogenous proteins in a broad variety of cell types and lines.¹²⁻¹⁴ The high sensitivity and quantitative capabilities of HiBiT allow easy implementation of this technology into HTS platforms for the identification of novel small molecule-based degraders, such as PROTACS and molecular glues.^{15,16} Furthermore, same-well multiplexing of cell health assays can yield additional information as to how these compounds are impacting cellular viability. This

application note shows parallel degradation and viability screening of several key IMiD molecular glue targets, IKZF1 (Ikaros), GSPT1 (G1 to S phase transition 1), and IKZF2 (Helios) with various IMiD drugs, using the BioSpa and Synergy Neo2 instrumentation.

Experimental

Nano-Glo HiBiT technology

Nano-Glo HiBiT from Promega Corporation (Madison, WI) offers a rapid and highly sensitive approach to tagging and detecting endogenous proteins in a broad variety of cell types and cell lines. This reporter system is based on split NanoLuc, and comprises an 11-amino acid peptide (HiBiT) that binds with very high affinity to an 18 kDa polypeptide (LgBiT). Efficient formation of a bright, luminescent complex enables highly sensitive and quantitative analysis of HiBiT-tagged proteins.¹⁷ The small size of HiBiT makes it an excellent choice for highly efficient and unobtrusive tagging of endogenous proteins by Cas9-mediated homology-directed repair using single-stranded donor oligonucleotide (ssODN) templates. Rapid and scalable detection of HiBiT-tagged proteins in cell lysates can be performed by addition of LgBiT protein and substrate in a lysis buffer. Alternatively, co-expression of LgBiT allows detection in live cells for real-time analysis of changes in protein abundance over extended periods of time, especially when combined with extended live cell substrates like Nano-Glo Endurazine, as seen in Figure 1. The high sensitivity of HiBiT, combined with flexible detection modalities, make HiBiT the ideal tool for investigating targeted degradation as a therapeutic approach. Furthermore, the simplicity of luminescence detection allows easy implementation of HiBiT into HTS platforms for the identification of novel small molecule-based degraders, such as PROTACS and molecular glues.^{15,16}

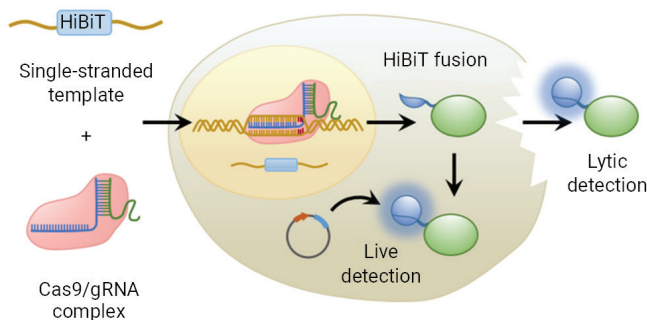


Figure 1. HiBiT protein-tagging technology. The genomic locus encoding the protein of interest can be tagged by homology-directed repair using Cas9 ribonucleoprotein (RNP) in combination with an ssODN repair template. The tagged protein can be detected either in a lytic end-point assay or by co-expressing LgBiT in live cells.

Instrumentation

The BioSpa 8 automated incubator can link Agilent BioTek readers or imagers together with Agilent BioTek washers and/or dispensers for full workflow automation of up to eight microplates. The Agilent BioTek BioSpa live cell analysis system provides temperature, gas, and humidity control during the assay run. The BioSpa system used in this application includes a BioSpa 8 automated incubator and a Synergy Neo2 hybrid multimode reader to automate kinetic live cell workflows in multiple plates over a period of 24 hours. The BioSpa 8 On-Demand mode software provides a simple, efficient interface for multiple reader protocols with start-time flexibility for each plate. The BioSpa 8 software integrates and schedules incubation, plate reading, and data analysis, while providing constant monitoring of all environmental conditions and processing steps. During an assay run, BioSpa 8 will transport and present the designated microplate to the Synergy Neo2 carrier, at which time the BioSpa 8 software will initiate the programmed plate-reader experiment in the Agilent BioTek Gen5 microplate reader and imager software. Once

complete, the data is electronically stored, and the plate is returned to the BioSpa 8.

The Synergy Neo2 multimode reader is designed for the screening laboratory, with speed and ultrahigh performance. Variable-bandwidth quad monochromators; sensitive, high-transmission, filter-based optics; laser time-resolved fluorescence (TRF); and up to four photomultiplier tubes (PMTs) provide rapid measurements. Synergy Neo2 uses independent optical paths, which ensure uncompromised performance in all detection modes, including absorbance, fluorescence, and luminescence. The reader uses barcode-labeled filter cubes to help streamline workflows and limit errors. Advanced environmental controls, including CO₂/O₂ control; incubation to 70 °C; and variable shaking, can support live cell assays.

Materials and methods

Jurkat cells stably expressing the LgBiT protein were further modified by inserting the HiBiT tag at the C-terminus of IKZF1, or the N-terminus of IKZF2, using CRISPR/Cas9. HEK293 cells stably expressing the LgBiT protein were similarly modified by inserting the HiBiT tag to the N-terminus of GSPT1. Cells expressing IKZF1-HiBiT were assayed in three 96-well plates (n=3 for each treatment or control condition), and cells expressing HiBiT-IKZF2 or HiBiT-GSPT1 were each assayed on a 384-well plate (n=4 for each treatment or control condition). HiBiT luminescence and CellTox Green fluorescence were measured every 30 minutes for 20 hours. Previously published experimental procedure and data analysis methods were followed for all assays.¹⁵

Results and discussion

Targeted degradation by several IMiD compounds can be observed with the IKZF1-HiBiT fusion protein, as shown in Figure 2. In this configuration, the HiBiT tag is situated at the C-terminus of the endogenous locus for IKZF1. Interestingly, despite the known efficacy, thalidomide shows only modest degradative activity, while the chemical derivatives of the basic structure are markedly more effective.

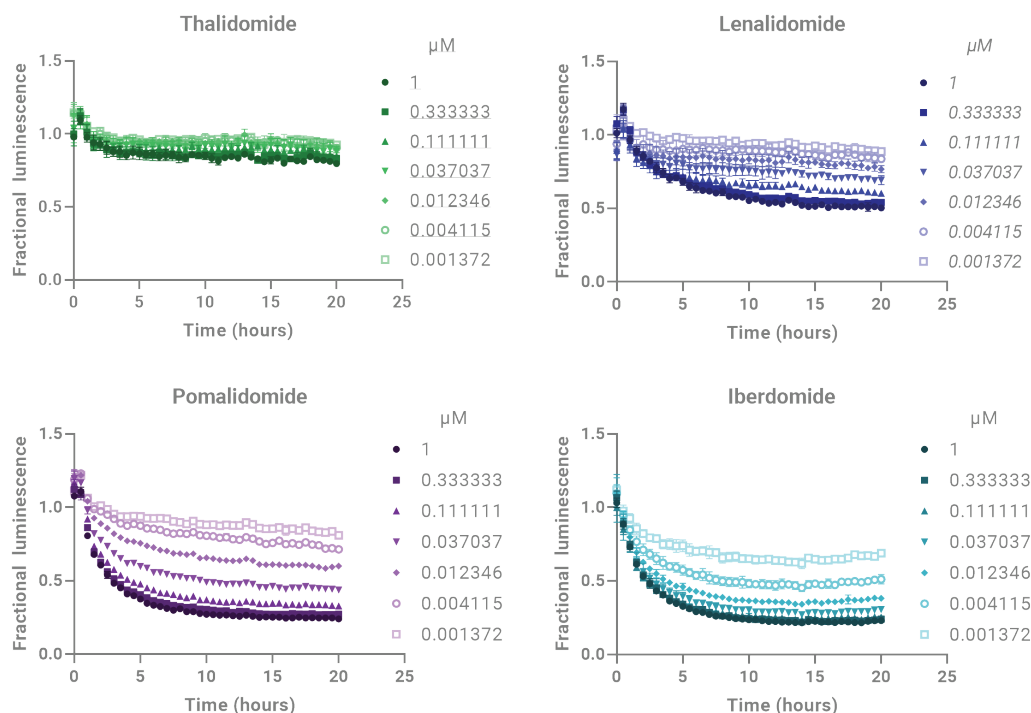


Figure 2. IKZF1-HiBiT live cell degradation. IKZF1-HiBiT KI Jurkat (LgBiT) cells (Promega) were plated in the presence of Nano-Glo Endurazine (Promega) and CellTox Green Dye (Promega) into 96-well plates at 100,000 cells/well, and treated with a concentration series of thalidomide, lenalidomide, pomalidomide, and iberdomide, or a DMSO control. Relative light unit (RLU) values were converted to fractional luminescence by dividing the raw RLU values of the treatment conditions by the raw RLU of the DMSO control for each time point. All compound concentrations are provided as μM . Data represent mean fractional RLU \pm SD (error bars) of technical triplicates.

The kinetic data for each compound at a fixed time point can be used to generate dose-response curves. By using a constrained Hill slope, four-parameter model, the potency of different compounds can be compared, as seen in Figure 3. Comparison of Dmax_{50} values indicates that iberdomide is 6 times more potent than pomalidomide, and 18 times more potent than lenalidomide in inducing degradation. In addition, iberdomide and pomalidomide were able to induce significantly more degradation as compared to lenalidomide (Figure 3).

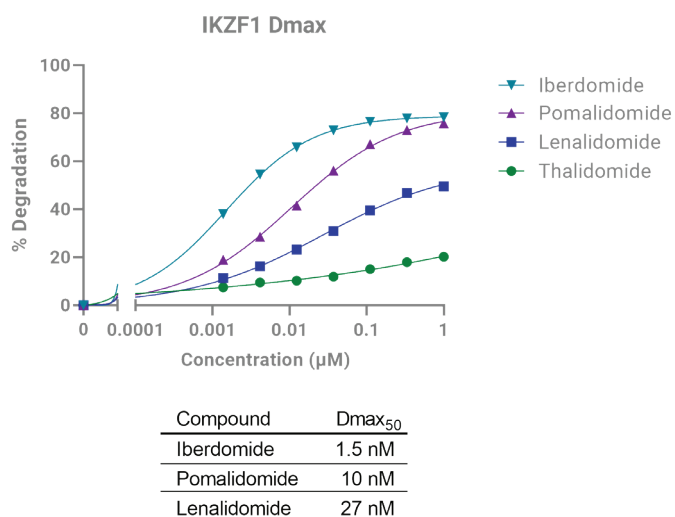


Figure 3. Percent degradation of treated Jurkat cells. Data presented in Figure 2 was used to determine degradation maximum (Dmax), defined as the lowest fractional RLU value achieved over time, and was determined for each treatment concentration. Dmax values were plotted against concentration and Dmax_{50} values were derived from four-parameter, nonlinear, regression curve fits for each compound treatment, as previously described.^{14,15}

When iberdomide, pomalidomide, and lenalidomide are directed against the endogenous HiBiT-tagged GSPT1 protein in modified HEK293 cells, very little degradation is observed, as seen in Figure 4. In this configuration, the HiBiT is situated at the N-terminus of the endogenous locus for GSPT1. The IMiD compound CC-885, a known potent inducer of Ikaros family zinc finger protein degradation, is also capable of causing degradation of the translation termination factor

GSPT1. This is observed in the kinetic luminescence plots of Figure 4A. The $D_{max_{50}}$ of this compound was determined to be 170 pM, as shown in Figure 4B.

The protein encoded by the IKFZ2, zinc finger protein Helios, is not targeted for degradation by the IMiDs tested. As demonstrated in Figure 5, very little change in the fractional luminescence is observed over the 20 hours of exposure, regardless of the compound.

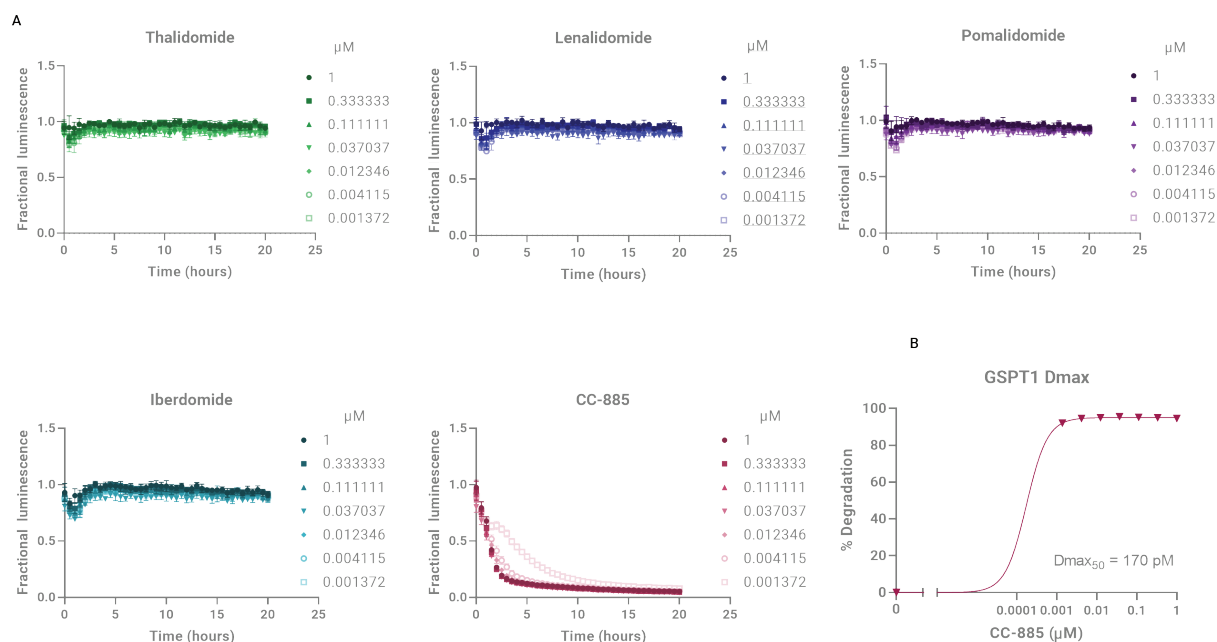


Figure 4. HiBiT-GSPT1 live cell degradation in HEK293 cells. (A) HiBiT-GSPT1 KI HEK293 (LgBiT) cells (Promega) were plated in the presence of Nano-Glo Endurazine and CellTox Green Dye into 384-well plates at 8,000 cells/well and treated with a concentration series of thalidomide, lenalidomide, pomalidomide, iberdomide, and CC-885, or a DMSO control. Fractional luminescence was calculated as outlined previously. All compound concentrations are provided as µM. Data represents the mean fractional RLU \pm SD (error bars) of technical quadruplicates. (B) Degradation maximum (D_{max}), defined as the lowest fractional RLU value achieved over time, was determined for CC-885 and used to derive a $D_{max_{50}}$ value.

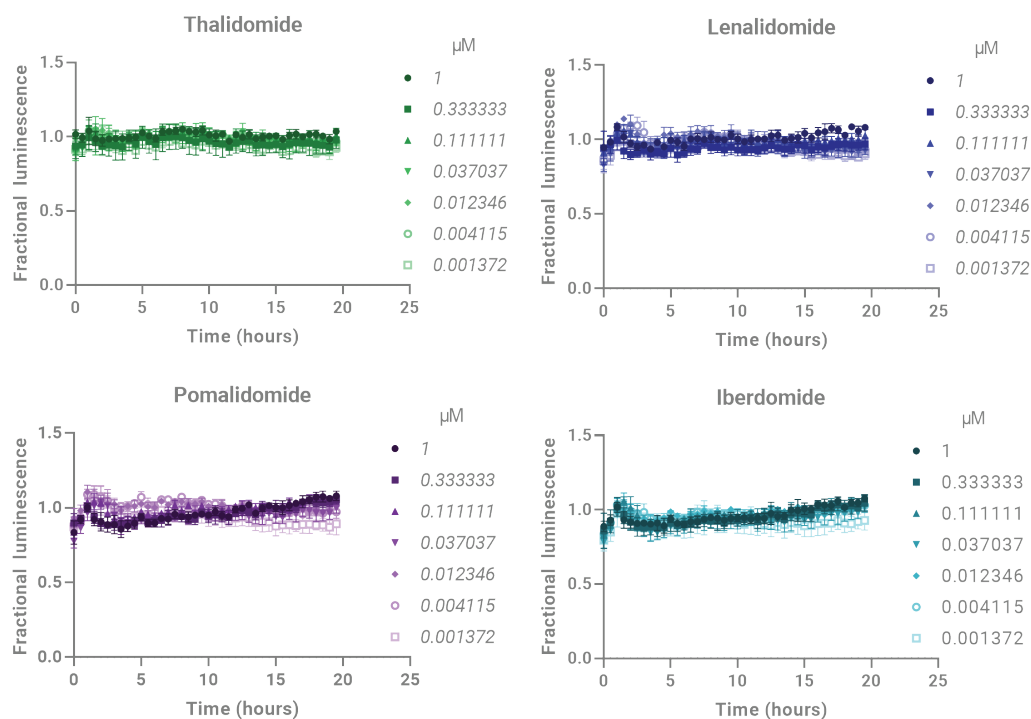


Figure 5. HiBiT-IKZF2 live cell degradation in Jurkat cells. HiBiT-IKZF2 KI Jurkat (LgBiT) cells (Promega) were plated in the presence of Nano-Glo Endurazine and CellTox Green Dye into 384-well plates at 50,000 cells/well, and treated with a concentration series of thalidomide, lenalidomide, pomalidomide, and iberdomide, or a DMSO control. Fractional luminescence was calculated as outlined previously. All compound concentrations are provided as μM . Data represents the mean fractional RLU \pm SD (error bars) of technical quadruplicates.

Cell health can be concurrently tested during the protein degradation assay. CellTox Green Dye is an impermanent cell dye that becomes highly fluorescent upon binding to nucleic acids. Healthy cells have an intact cell membrane, which effectively excludes the dye, while cells compromised by toxic insults will have a damaged cell membrane that cannot exclude the dye. Compounds that are cytotoxic would

be expected to produce increased fluorescence over time as compared to nontoxic compounds. The representative data presented in Figure 6 demonstrates that the highest concentration of IMiDs (1 μM) does not result in increased fluorescence in either Jurkat or HEK293 cells relative to the untreated negative control, and therefore does not impact cell health at these tested concentrations.

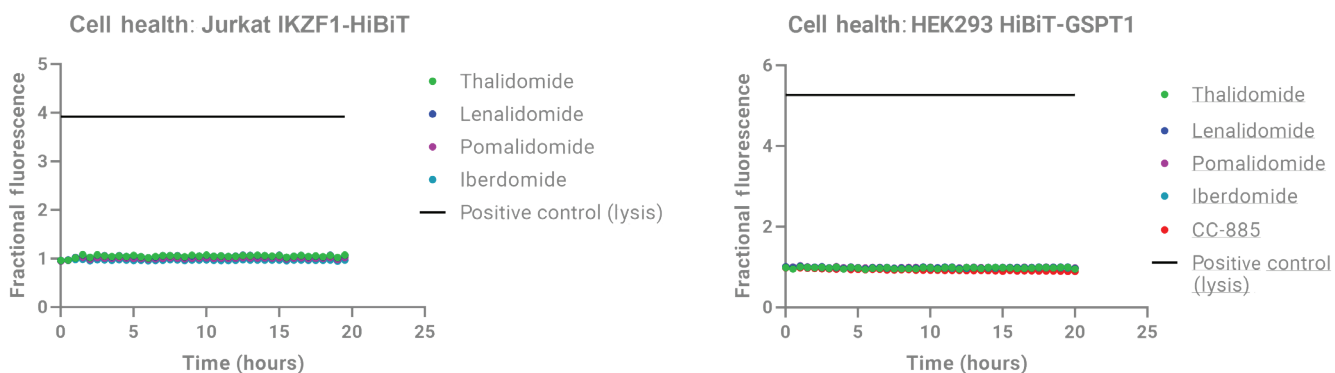


Figure 6. Multiplexing cell health in Jurkat-*IKZF1*-HiBiT and HEK293 HiBiT-*GSPT1* cells. The CellTox Green cytotoxicity assay was multiplexed with the kinetic degradation data shown in Figures 2 through 5, as previously described.¹⁵ Representative data is shown for Jurkat *IKZF1*-HiBiT and HEK293 HiBiT-*GSPT1* cells respectively. RFU data was normalized through conversion to fractional RFU by dividing the raw RFU values of the treatment conditions by the raw RFU values of the DMSO control for each time point. The relative maximum lysis control value was calculated by dividing the raw RFU values for the cell lysis control (100 μ g/mL digitonin) by the raw RFU value of the DMSO control, and is provided on each graph for reference. Shown are representative results for treatment with the highest compound concentration (1 μ M) used for each experiment. Data represents the mean fractional RFU \pm SD of technical quadruplicates.

Multiplexing with a fluorescence cell viability assay demonstrated that compound treatment did not result in significant cell death over the time frame tested in this experiment. This suggests that the observed decrease in target protein abundance is compound-specific degradation, and not a consequence of cell death.

These data indicate that the BioSpa 8 in conjunction with the Synergy Neo2 can reliably automate HiBiT-tagged protein degradation assays. Several different IMiD compounds were successfully tested for activity against different HiBiT-modified cell lines. These results match those of previously published data, where the plates were run manually without the use of a robotic incubator.^{3,4,15}

This instrument combination allows multiple plates to be run concurrently. The On-Demand BioSpa software allows staggering at the start of multiple assay plates, enabling the robot to shuttle plates to the multimode reader in succession, while maintaining uniform read-to-read timing. Between reads, the plate is returned to the environmentally controlled incuba-

tor. Normally, a single plate would occupy the reader for the entirety of the kinetic assays. Besides multiple plates, this system can accommodate different plate formats. Both 96- and 384-well microplates were used concurrently in these experiments. In addition to controlling assay timing, the BioSpa 8 software can attach specific reader protocol files to specific plates. The ability to run multiple plates concurrently improves throughput dramatically and reduces personnel costs. For example, without the BioSpa 8, running four separate plates would require four sequential 20-hour runs, with four discrete assay preparations. The ability to run multiple plates concurrently requires only one assay preparation, which eliminates some of the potential assay variability and provides better assay statistics. Alternatively, the assays could be carried out manually, where a researcher would be required move individual plates from a tissue culture incubator to the reader carrier and initiate the detection step, over the same 20-hour time period.

Conclusion

For all data, the differences in degradation amongst the IMiD compounds for any given HiBiT CRISPR target, as well as the family member specificity, matches what has previously been published.^{3,4,15} Multiplexing with a fluorescence cell viability assay demonstrates that compound treatment did not result in significant cell death over the time frame tested in this experiment. This suggests that the observed decrease in target protein abundance is compound-specific degradation and is not a consequence of cell death. Coupling the HiBiT CRISPR technology for degradation screening with the Agilent BioTek BioSpa 8 automated incubator On-Demand method allowed for multiplexed luminescence and fluorescence data collection from all five assay plates in parallel. This saved significant time in experimental setup and execution. Use of the Agilent BioTek Synergy Neo2 hybrid multimode reader resulted in generation of highly robust and reproducible data for both the HiBiT luminescence and the CellTox Green fluorescent live cell assays.

References

1. Deshaies, R.J. Protein Degradation: Prime Time for PROT-ACs. *Nat Chem Biol* **2015**, *11*:634-635.
2. Lai, AC; Crews, CM. Induced Protein Degradation: An Emerging Drug Discovery Paradigm. *Nat Rev Drug Discov* **2017**, *16*:101-114.
3. Chamberlain, PP; D'Agostino, LA; Ellis, JM; Hansen, JD; Matyskiela, ME; McDonald, JJ; Riggs, JR; Hamann, LG. Evolution of Cereblon-Mediated Protein Degradation as a Therapeutic Modality. *ACS Med Chem Lett* **2019**, *10*:1592-1602.
4. Chamberlain, PP; Hamann, LG. Development of Targeted Protein Degradation Therapeutics. *Nat Chem Biol* **2019**, *15*:937-944.
5. Ito, T; Ando, H; Suzuki, T; Ogura, T; Hotta, K; Imamura, Y; Yamaguchi, Y; Handa, H. Identification of a Primary Target of Thalidomide Teratogenicity. *Science*. **2010**, *327*(5971):1345–50.33.
6. Lu, G; Middleton, RE; Sun, H; Naniong, M; Ott, CJ; Mitsiades, CS; Wong, KK; Bradner, JE; Kaelin, WG Jr. The Myeloma Drug Lenalidomide Promotes the Cereblon-Dependent Destruction of Ikaros Proteins. *Science*. **2014**, *343*(6168):305–9.34.
7. Kronke, J; Udeshi, ND; Narla, A; Grauman, P; Hurst, SN; McConkey, M; Svinkina, T; Heckl, D; Comer, E; Li, X; et al. Lenalidomide Causes Selective Degradation of IKZF1 and IKZF3 in Multiple Myeloma Cells. *Science*. **2014**, *343*(6168):301–5.35.
8. Stewart, AK. Medicine. How Thalidomide Works Against Cancer. *Science*. **2014**, *343*(6168):256–7.
9. Fischer, ES; Bohm, K; Lydeard, JR; Yang, H; Stadler, MB; Cavadini, S; Nagel, J; Serluca, F; Acker, V; Lingaraju, GM; et al. Structure of the DDB1-CRBN E3 Ubiquitin Ligase in Complex with Thalidomide. *Nature*. **2014**, *512*(7512):49–53.43.
10. Chamberlain, PP; Lopez-Girona, A; Miller, K; Carmel, G; Pagarigan, B; Chie-Leon, B; Rychak, E; Corral, LG; Ren, YJ; Wang, M; et al. Structure of the Human Cereblon-DDB1-Lenalidomide Complex Reveals Basis for Responsiveness to Thalidomide Analogs. *Nat Struct Mol Biol*. **2014**, *21*(9):803–9.44.
11. Petzold, G; Fischer, ES; Thoma, NH. Structural Basis of Lenalidomide-Induced CK1alpha Degradation by the CRL4 Ubiquitin Ligase. *Nature*. **2016**, *532*(7597):127–30.
12. Schwinn, MK; Machleidt, T; Zimmerman, K; Eggers, CT; Dixon, AS; Hurst, R; Hall, MP; Encell, LP; Binkowski, BF; Wood, KV. CRISPR-Mediated Tagging of Endogenous Proteins with a Luminescent Peptide. *ACS Chem Biol* **2018**, *13*:467-474.
13. Schwinn, MK; Steffen, LS; Zimmerman, K; Wood, KV; Machleidt, T. A Simple and Scalable Strategy for Analysis of Endogenous Protein Dynamics. *Sci Rep* **2020**, *10*:8953.
14. Riching, KM; Mahan, S; Corona, CR; McDougall, M; Vasta, JD; Robers, MB; Uhr, M; Daniels, DL. Quantitative Live-Cell Kinetic Degradation and Mechanistic Profiling of PROTAC Mode of Action. *ACS Chem Biol* **2018**, *13*:2758-2770.
15. Riching, KM; Mahan, SD; Uhr, M; Daniels, DL. High-Throughput Cellular Profiling of Targeted Protein Degradation Compounds using HiBiT CRISPR Cell Lines. *J Vis Exp* **2020**.
16. Daniels, DL; Riching, KM; Uhr, M. Monitoring and Deciphering Protein Degradation Pathways Inside Cells. *Drug Discov Today Technol* **2019**, *31*:61-68.
17. Dixon, AS; Schwinn, MK; Hall, MP; Zimmerman, K; Otto, P; Lubben, TH; Butler, BL; Binkowski, BF; Machleidt, T; Kirkland, TA; et al. NanoLuc Complementation Reporter Optimized for Accurate Measurement of Protein Interactions in Cells. *ACS Chem Biol* **2016**, *11*:400-408.

www.agilent.com/lifesciences/biotek

For Research Use Only. Not for use in diagnostic procedures.

RA44616.551712963

This information is subject to change without notice.

© Agilent Technologies, Inc. 2022
Published in the USA, February 28, 2022
5994-4599EN

